INNSPUB

RESEARCH PAPER

Mapping of arid rangeland vegetation types using satellite data (study site: Ameri, Iran)

Shahram Yousefi Khanghah[*]

Department of Range and Watershed Management, Behbahan Khatam Alanbia Tecnology of University, Behbahan, Iran

Abstract

Remote sensing assessment is used along with field data to enhance sampling and site representation. The research was carried out in Ameri region located between 50° 05´ to 50° 16´ east longitude and 30° 03´ to 30° 13´ north latitude in south west of Iran, as a dry Climate and located in the coastal region with 15915 hectare area. The aim of the present research was to produce rangeland vegetation types using satellite data. Geometric corrections of images were applied using ground control points (GCP) and geo-referenced images with root mean square error (RMSE) less than one pixel, then images Co-registered together with RMSE less than 0.2 pixels. The atmospheric corrections of images were applied using Cost method. Image spatial resolution enhanced using fusion with a panchromatic band. Images classified using maximum likelihood (ML) algorithm of supervised classification with 100 training area, and produced five rangeland vegetation types, then accuracy of produced maps determined with ground truth samples. The results show that both sensors can produce suitable vegetation type's map in study area, and ML classification method able to delineate rangeland vegetation type's map with acceptable precision. As a result we imply that visual interpretation and manual mapping will be used to delineate vegetation type's maps of arid rangelands.

*Corresponding Author: Shahram Yousefi Khanghah ✉ shahramyousefi@gmail.com

Introduction

Rangeland is an economically and culturally important enterprise in Iran, as it is elsewhere in the world. Vegetation type's map is very important in regional and national planning of rangeland management. Vegetation types refer to specific plant community in one place. Usually every vegetation type specified with one land type, though that is possible more than one types exist on one land type; dominant species is operative factor in separation of vegetation types (Mesdaghi, 1999). To effectively manage rangelands it is important to assess ecosystem productivity and biomass production (Running *et al.*, 2004).

Remote sensing (RS) and geographic information system (GIS) have been widely applied in identifying and analyzing land use/cover change. Remote sensing assessment is used along with field data to enhance sampling and site representation (Booth *et al.*, 2005). RS can provide multi-temporal data than can be used to quantify the type, amount and location of land use change. GIS provides a flexible environment for displaying, storing and analyzing digital data necessary for change detection (Wu *et al.*, 2006). In remote sensing technology, classification as a common image processing technique is implemented to derive data regarding land use/cover types (Vogelmann *et al.*, 2001). In supervised classification, spectral signatures are collected from training sites in the image by digitizing various polygons overlaying different land use types. The spectral signatures are then used to classify all pixels in the scene. The supervised classification is generally followed by knowledge-based expert classification systems depending on reference maps to improve the accuracy of the classification process (Xiaoling *et al.*, 2006).

Weeks *et al.* (2013) compared four remote sensing methods to detect changes in New Zealand's grasslands (image differencing, normalized difference vegetation index (NDVI) differencing post-classification and visual interpretation. The visual interpretation resulted in the best classification

results, when compared with ground truth data (overall accuracy 98%). Amiri and Yeganeh (2012) evaluated vegetation indices for preparing vegetation cover percentage map using ASTER in semi-arid lands of Ghareh Aghaj watershed, central Iran. Generally NDVI and SAVI indices provided accurate quantitative estimation of the parameters. Therefore, it is possible to estimate cover and production as important factors for rangeland monitoring using ASTER data. Shoshany and Karnibad (2011) investigated the two approaches to biomass mapping of shrub lands across sub-humid and arid transition zones, including relationships between biomass and precipitation from sites in the Mediterranean Basin, California, Namibia and Mongolia, and representing NDVI-based models for biomass estimation on a regional scale. These results support the possibility that the modified model can be used to map biomass across wide Mediterranean and desert fringe ecosystems. DeRose *et al.* (2011) investigated potential use of visible and near infrared of ASTER in monitoring vegetation recovery following volcanic eruptions on Mt. Pinatubo, the Philippines. They mentioned that NDVI derived from ASTER imagery can be used to discriminate and map areas of land that have gained or lost vegetation cover over relatively short periods. Yüksel *et al.* (2008) performed Land Use/cover Classification of Eastern Mediterranean Landscapes in Kahramanmaras, Turkey using ASTER Imagery. The results indicated that using the surface reflectance data of ASTER sensor imagery can provide accurate and low-cost cover mapping as a part of CORINE land cover project.

The aim of this study was to producing rangeland vegetation type's map using LISS III and ASTER satellite sensors in arid rangeland of Ameri area, south western of Iran. Coastal rangeland of study area is important because of forage production, soil conservation, ecotourism, and bird nest values.

Material and methods

Study area

The research was carried out in Ameri region located between 50° 05´ to 50° 16´ east longitude and 30° 03´ to 30° 13´ north latitude in Bushehr province at south west of Iran (Fig.1) as a dry Climate and located in the coastal region with 15915 hectares area. Average annual precipitation is 224.6 mm and average annual temperature is 25.4 Co. The area is steppe, consisting primarily of native and non-native species including grasses (*Aelorupus lagopoeides, Stipa capensis)*, forbs (*Plantago cylindrical, Centaurea Bruguierana*), and many shrub (*Halocnemum strobilaceum, Gymnocarpus decandera, Astragalus fasiculifolius, Halotamnus iranica, Arthrochnemum machrostachyum*). Sheep and goat grazing is the primary usage of the study area rangeland. Land uses include rangeland (95.7%), afforest (3.2%), agriculture (0.9%) and residential (0.2%).
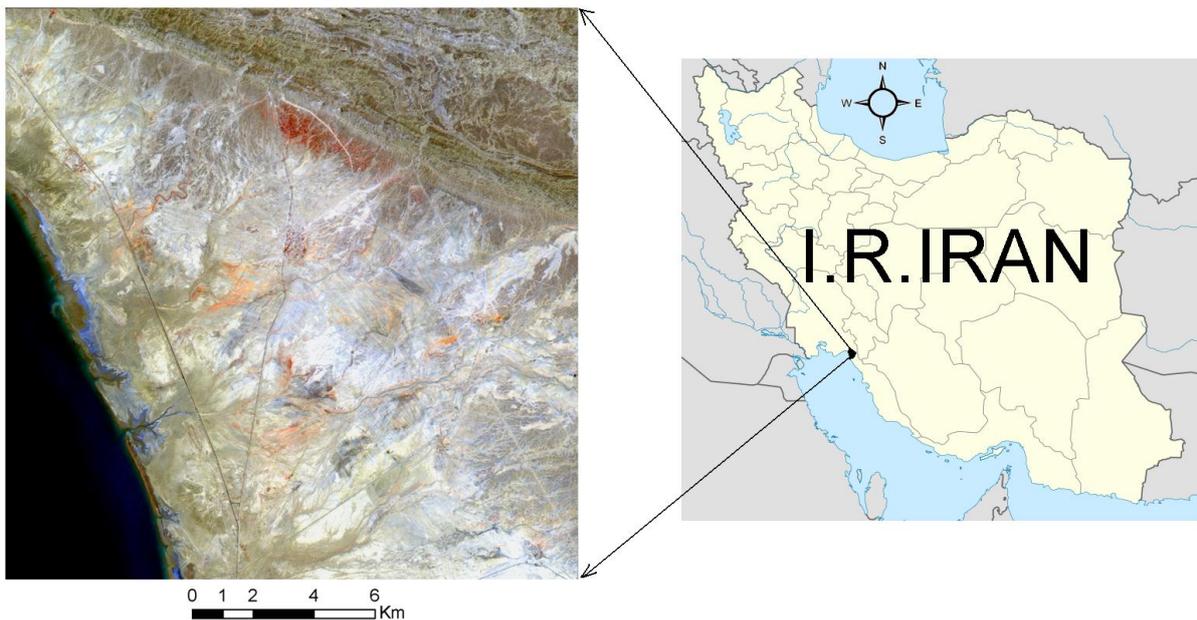
Fig. 1. Location of study site in Iran.

Satellite data

Topography map (with 1:25000 scale) and geology map (with 1:100000 scale) of study area was acquired from Iranian national cartographic center (NCC) and geological survey of Iran (GSI), respectively. Indian Remote Sensing Resource-Sat/P6 linear imaging self-scanning sensor (LISS) III multispectral imagery (23.5 m × 23.5 m pixels) was acquired for the study area on 07 February 2011 and advanced spaceborne thermal emission and reflection radiometer (ASTER) multispectral imagery (15 m × 15 m pixels) was acquired for the study area on 10 January 2011. These data were selected because of their low cloud cover.

Field data

The primary vegetation map was delineated using a geology and topography maps, then field studies and sampling started in February 2011. In each vegetation type 20 training area (100 training area in total) used to producing rangeland vegetation types map, and 25 ground truth samples used to determining of the accuracy of produced maps. Coordinate of training areas recorded by GPS (Garmin eTrex Vista CX).

Preprocessing of satellite data

The images georeferenced using ground control points extracted from topography map 1:25000 and GPS (with RMSE less than 1 pixel), and projected in UTM Zone 39 North with WGS 1984 datum. Image was corrected for atmospheric effects using the Cost model and input parameters reported in the metadata supplied by IRS and ASTER Images Corporation. It

incorporates all of the elements of the Dark Object Subtraction model (for haze removal) plus a procedure for estimating the effects of absorption by atmospheric (Chavez, 1996) gases and Rayleigh scattering. Atmospheric correction was performed with IDRISI Taiga (v16.03) using the ATMOSC module. For pan sharpening to be effective, the images of interest must be closely aligned. The georeferencing information that comes with the imagery is typically not accurate enough for this purpose. Instead, we select tie points marking the same features on both images, and then warps one image based on these tie points to match the base image (with RMSE less than 0.2 pixels). We used fusion for merge a low-resolution multispectral images with a high-resolution panchromatic image (Campbell and Wynne, 2011). Gram-Schmidt pan sharpening methods with nearest neighbor resampling used for Image Sharpening.

Classification

In first step delineate the rangeland boundary and masked the other land uses/covers. Supervised classification clusters pixels in an image into classes based on user-defined training data. The training data can come from Polygons and points from existing vector layers or shape files or create on a loaded image. Once we defined the classes that we want mapped in the output, then we select the training data. We defined five classes in the study area and select 30 training data in each class. Then the separability of training data calculated using Jeffries-Matusita method. These values range from 0 to 2.0 and indicate how well the selected training data pairs are statistically separate. Values greater than 1.9 indicate that the selected training data pairs have good separability. The Maximum likelihood algorithm used for supervised classification. ML Assumes that, the statistics for each class in each band are normally distributed, and calculates the probability that a given pixel belongs to a specific class. Each pixel is assigned to the class that has the highest probability (Richards, 1999). ML classification calculates the following discriminant functions for each pixel in the image:

$$g_i(x) = \ln p(\omega_i) - \tfrac{1}{2}\ln |\Sigma_i| - \tfrac{1}{2}(x - m_i)^T \Sigma_i^{-1}(x - m_i)$$

Where:

i = the ith class

x = n-dimensional data (where n is the number of bands)

$p(\omega i)$ = probability that a class occurs in the image and is assumed the same for all classes

$|\Sigma i|$ = determinant of the covariance matrix of the data in a class

$\Sigma i{-1}$ = the inverse of the covariance matrix of a class

mi = mean vector of a class

Majority analysis (3×3 pixel) used to change single pixels within a large single class to that class.

Accuracy assessment

Accuracy assessment is an important final step in both unsupervised and supervised classifications. Its purpose is to quantify the likelihood that what you mapped is what you will find on the ground. The confusion (contingency) matrix used to show the accuracy of a classification result by comparing a classification result with ground truth information. In each case, we calculate overall accuracy and kappa coefficient. The overall accuracy is calculated by summing the number of pixels classified correctly and dividing by the total number of pixels (Jensen, 1986). The Kappa (κ) Index of agreement is similar to a proportional accuracy figure (and thus the complement of proportional error), except that it adjusts for chance agreement. Kappa is essentially a statement of proportional accuracy, adjusted for chance agreement (Campbell and Wynne, 2011). Its value varies from 0 to 1.

Results and discussion

Rangelands included five vegetation types (Table 1), which numbered from shoreline (1) to height (5). The separability of training data (Table 2) was good. Type 1 has most separability (1.97) from types 3 and 4. Type 1 has only one specie (Halocnemum strobilaceum), and differ from other types because of less vegetation cover, that effect on reflectance. Type 3 has least separability (1.90) from type 4. Type 5 have a different vegetation

type (mostly shrub) and height (highest) and slope (steep), so it separate easy from other types. Vegetation maps produced from ML classification of LISS III and ASTER presented in fig. 2 and 3. Result show that type 3 have most area (Table 3) in rangeland at both produced map; LISS III (44.8%) and ASTER (44.4.6%). type 1 has least area at both produced maps; LISS III (5.5%) and ASTER (5.4%).

**Table 1.** Properties of vegetation types in study area.

ID	Abbreviation	Vegetation types full name	Cover (%)	Area (hectare)	Percent (%)
1	Ha.st	*Halocnemum strobilaceum*	12.8	620	4.1
2	Ha.st– Pl.cy	*Halocnemum strobilaceum – Plantago cylindrica*	27.6	4321	28.4
3	Ha.ir – As.fa	*Halotamnus iranica - Astragalus fasiculifolius*	34.4	8441	55.4
4	Gy.de – Pl.mu	*Gymnocarpus decandera - Platycheat munronifolia*	25.5	1602	10.5
5	Ar.ma	*Arthrochnemum machrostachyum*	27.5	250	1.6
Total				15234	100

Table 2. Separability of training data calculated using Jeffries-Matusita method.

Vegetation types	Type 1		Type 2		Type 3		Type 4		Type 5	
sensors	LISSIII	ASTER	LISSIII	ASTER	LISSIII	ASTER	LISSIII	ASTER	LISSIII	ASTER
Type 1	2.00	2.00	1.94	1.93	1.97	1.96	1.97	1.97	1.96	1.96
Type 2	1.94	1.93	2.00	2.00	1.93	1.92	1.95	1.95	1.97	1.96
Type 3	1.97	1.96	1.93	1.92	2.00	2.00	1.91	1.90	1.95	1.95
Type 4	1.97	1.97	1.95	1.95	1.91	1.90	2.00	2.00	1.93	1.92
Type 5	1.96	1.96	1.97	1.96	1.95	1.95	1.93	1.92	2.00	2.00

Table 3. Area (hectares) of vegetation types in study area.

Sensor	ML Classification ASTER		ML Classification LISS III	
Vegetation types	area	percent	area	Percent
1	822.6	5.4	837.9	5.5
2	3366.8	22.1	3135.4	20.7
3	6763.9	44.4	6824.8	44.8
4	4037	26.5	4021.8	26.6
5	243.7	1.6	396.1	2.6
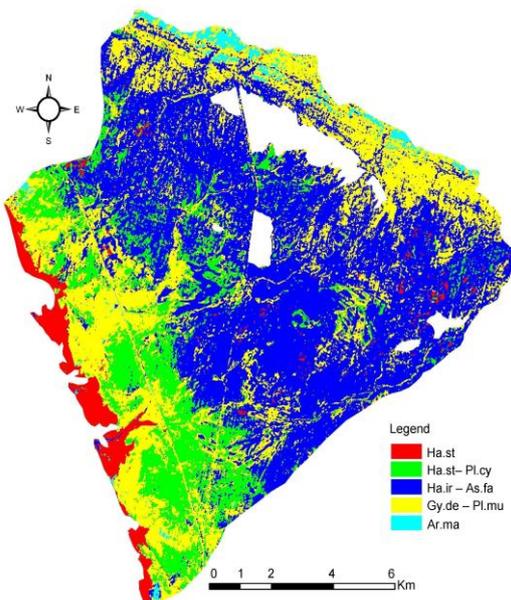
Fig. 2. Rangeland vegetation types produced by ML classification of LISS III.
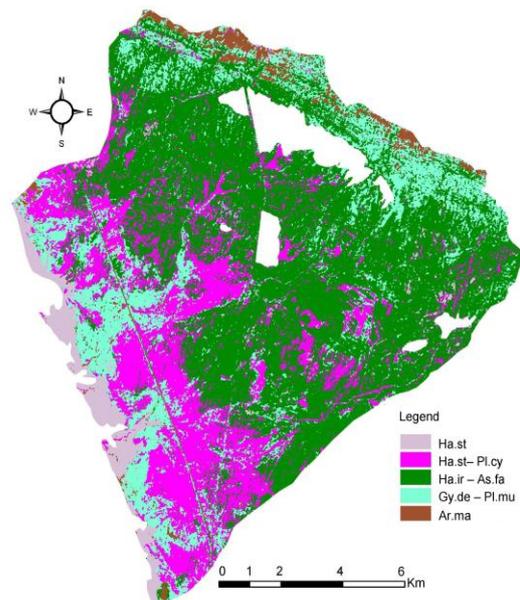
Fig. 3. Rangeland vegetation types produced by ML classification of ASTER.

Both images produced suitable vegetation types map and didn't more different between produced vegetation type's maps. The combination of ASTER and IRS bands has the most information content, Additionally, NDVI of ASTER and IRS has the same effect on enhancement of bare soil and vegetation covers (Shirazi *et al.*, 2011). Insomuch pan sharpening of low-resolution multispectral images LISS III (24m×24m) and ASTER (15m×15m) with panchromatic (5.8m×5.8m) enhanced the ground resolution (pixel size) of images. Using of fused images of IRS Pan and LISS III data could better classified forest and non-forest areas than other images with 89.5% overall accuracy and 0.72 Kappa coefficient (Shataee *et al.*, 2008); that confirmed in this study. Also the precision of LISS III is a slightly better than ASTER, because the imaging date of LISS III was near to field sampling date; and the vegetation cover percent is verisimilitude. ASTER imagery, when captured at a similar time of year, can be used to discriminate and map areas of land that have gained or lost vegetation cover over relatively short periods (De Rose *et al.*, 2011). Results showed that the classified images obtained from two sensors by comparison after classification method had a high accuracy. Overall accuracy and kappa coefficient of ML classification was 91.18% and 0.864 for LISS III and, 83.54% and 0.786 for ASTER, respectively. LISS III sensor has higher accuracy from ASTER, because the imaging date was near to field sampling date. Lillesand *et al.* (2004) implied that the maximum likelihood is most accurate and most used method among the supervised classification methods; that confirmed in this study.

The satellite images cannot determine exactly the rangeland vegetation type boundary in the study area; therefore, the produced maps completed with visual interpretation of images and the final vegetation map produced (Fig. 4). While research progresses, visual interpretation and manual mapping used to monitor land-use/cover change in grasslands will be used. The visual interpretation resulted in the best classification results, with a 98% overall accuracy when compared

with ground truth data (Weeks *et al.*, 2013). Our study shows that it is difficult to differentiate between rangeland types in rangeland. This is supported by Vescovo *et al.* (2009); they conducted a preliminary study of mapping biomass and cover in New Zealand grasslands using 2003/2004 Landsat imagery. As a result, ML classification method was able to delineate arid rangeland vegetation type's map with acceptable precision. Furthermore, this method was unable to provide exact precision information regarding the nature of vegetation types.

Conclusion

This study confirms the usability of satellite images for interpretation of spectral signature to detect vegetation maps of arid rangelands of Iran. The results show that both sensors can produce suitable vegetation types map in study area, and didn't more different between produced vegetation type's maps of two sensors. The results imply that visual interpretation and manual mapping will be used to delineate vegetation type's maps in arid rangelands. This was due to the complexity and variability in the spatial patterns of the rangeland ecosystems, making the spectral reflectance indistinct. Further research is needed in this arid rangeland to develop the other classification methods to vegetation type's maps detection.
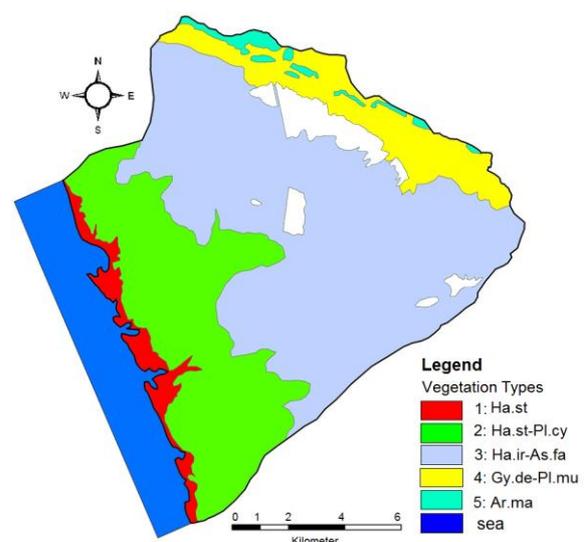
Fig. 4. Rangeland vegetation types map produced by visual interpretation.

References

Amiri F, Yeganeh H. 2012. Evaluation of vegetation indices for preparing vegetation cover percentage in semi-arid lands of central Iran (case study: Ghareh Aghaj watershed). Range and watershed management, **65 (2)**, 175-18.

Campbell JB, Wynne RH. 2011. Introduction to remote sensing, fifth Edition, Guilford Press, New York. 718 p.

Chavez PS. 1996. Image-Based atmospheric corrections revisited and improved, photogrammetric engineering and remote sensing, **62**, 9, 1025-1036.

DeRose RC, Oguchi T, Morishima W, Collado M. 2011. Land cover change on Mt. Pinatubo, the Philippines, monitored using ASTER VNIR, remote sensing, **32 (24)**, 9279–9305.

Freeman EA, Moisen GG. 2008. A comparison of the performance of threshold criteria for binary classification in terms of predicted prevalence and kappa. Ecological modeling, **217 (1)**, 48–58.

Jensen R. 1986. Introductory digital image processing, Prentice-Hall, Englewood Cliffs, New Jersey, p. 379.

Lillesand TM, Kiefer RW, Chipman W. 2004. Remote sensing and image interpretation. 5th edition, New York, Jhon Willey and Sons, 763 p.

Mesdaghi M. 1999. Range management in Iran. University of Imam Reza press, Mashahd, Iran. 259p.

Richards JA. 1999. Remote sensing digital image analysis, Springer, Verlag, Germany, 240 p.

Shataee JS, Najjarlou S, Jabbary S, Moaiery H. 2008. Investigation on capability of multi spectral and fused LANDSAT7 and IRS1D data for forest extent mapping. Agriculture science and natural resource. **14 (5)**, 13-22.

Shirazi M, Matinfar HR, Nematolahi MJ, Zehtabian GR. 2011. Comparison of information content of Aster and LISS-III bands in arid areas (case study: Damghan playa). Applied RS & GIS techniques in natural resource science. **1 (1)**, 31-47.

Shoshany M, Karnibad L. 2011. Mapping shrubland biomass along Mediterranean climatic gradients: The synergy of rainfall-based and NDVI-based models. Remote sensing, **32 (24)**, 9497–9508.

Vescovo L, Tuohy M, Gianelle D. 2009. A preliminary study of mapping biomass and cover in NZ grasslands using multispectral narrow-band data. In: Jones S, Reinke K, eds. Innovations in remote sensing and photogrammetry. Springer, Heidelberg, Germany, pp. 281–90.

Vogelmann JE, Helderb D, Morfitta R, Choatea MJ, Merchantc JW, Bulley H. 2001. Effects of Landsat 5 thematic mapper and Landsat 7 enhanced thematic mapper plus radiometric and geometric calibrations and corrections on landscape characterization. Remote sensing of environment, **78**, 55-70.

Weeks ES, Gaelle A, Ausseil E, Shepherd JD, Dymond JR. 2013. Remote sensing methods to detect land-use/cover changes in New Zealand's 'indigenous' grasslands, New Zealand geographer, **69 (1),** 1-13.

Wu Q, Li HQ, Wang RS, Paulussen J, He Y, Wang M, Wang BH, Wang Z. 2006. Monitoring and predicting land use change in Beijing using remote sensing and GIS, Landscape and urban planning, **78**, 322-333.

Xiaoling C, Xiaobin C, Hui L. 2006. Expert classification method based on patch-based neighborhood searching algorithm. Geo-spatial information science, **10 (1)**, 37-43.

Yüksel A, Akay A, Gundogan R. 2008. Using ASTER imagery in land use/cover classification of eastern mediterranean landscapes According to CORINE land cover project. Sensors, **8(2),** 1237-1251.